10-24-2007

Microimprinting and ferroelectric properties of poly(vinylidene fluoride-trifluoroethylene) copolymer films

Lei Zhang
University of Nebraska - Lincoln

Stephen Ducharme
University of Nebraska, sducharme1@unl.edu

Jiangyu Li
University of Washington, jjli@uw.edu

Microimprinting and ferroelectric properties of poly(vinylidene fluoride-trifluoroethylene) copolymer films

Lei Zhang
Department of Mechanical Engineering, University of Washington, Seattle, Washington 98195-2600, USA and Department of Physics and Astronomy and Nebraska Center for Materials and Nanoscience, University of Nebraska, Lincoln, Nebraska 68588-0111, USA

Stephen Ducharme
Department of Physics and Astronomy and Nebraska Center for Materials and Nanoscience, University of Nebraska, Lincoln, Nebraska 68588-0111, USA

Jiangyu Li[a)]
Department of Mechanical Engineering, University of Washington, Seattle, Washington 98195-2600, USA

(Received 9 August 2007; accepted 29 September 2007; published online 24 October 2007)

Poly(vinylidene fluoride-trifluoroethylene) [P(VDF-TrFE)] copolymer films have been patterned by microimprinting with excellent quality of pattern transferring. Ferroelectricity of the imprinted films has been confirmed by ferroelectric hysteresis and surface potential measurement, and very good correlation is observed between remnant polarization and surface potential of the imprinted films. Imprinted P(VDF-TrFE) films show high remnant polarization and high poling-induced surface potential when the imprinting temperature is around 140 °C, suggesting that 140 °C is the optimal imprinting temperature for P(VDF-TrFE) films. The patterned ferroelectric P(VDF-TrFE) films can be used for a wide range of applications. © *2007 American Institute of Physics*.
[DOI: 10.1063/1.2800803]

There is great excitement on polyvinylidene fluoride (PVDF)-based ferroelectric polymers in the past decades, thanks to their scientific significance and technological implications.[1–5] From both scientific and technological points of view, it is highly desirable to pattern PVDF-based ferroelectric polymer films with feature size down to micro- or nanometer scale. This would not only allow us to probe ferroelectricity and ferroelectric phase transition in one and even zero dimensions but also enable micro- and nanoscale ferroelectric arrays for various device applications. Different techniques[6–8] have been applied to pattern inorganic and organic ferroelectric micro- and nanostructures,[9–12] including focused ion beam milling, electron-beam direct writing, soft lithography, and imprint lithography. For example, a temperature-controlled capillary molding has been applied to pattern α- and γ-phase PVDF homopolymer films,[13] and nanoimprint lithography has been applied to pattern α-phase PVDF homopolymer.[14] Localized pressure has also been used to transform the paraelectric α-phase PVDF into the ferroelectric γ phase during microimprinting.[15]

It is well known that the potential applications of PVDF mainly come from the piezoelectricity and ferroelectricity of its polar β phase,[16] especially P(VDF-TrFE) copolymers. Yet, there are very few works reported on the patterning of β-phase P(VDF-TrFE) copolymer films, to the best knowledge of the authors. Self-organizing ferroelectric nanomesas and nanowells were reported in Langmuir-Blodgett P(VDF-TrFE) films annealed above the ferroelectric phase transition temperature,[17–20] but the resulting structure is irregular in morphology and distribution, not suitable for device applications. A white light synchrotron radiation source has been used to photoetch and pattern a small area of P(VDF-TrFE) film,[21] but such a process induces substantial chemical modification in P(VDF-TrFE) chain structure, and it is not clear if such patterned P(VDF-TrFE) films still exhibit good ferroelectricity essential for their applications.

Among all the techniques mentioned, micro- and nanoimprintings are especially attractive for patterning ferroelectric polymers over large areas, with potential to reach feature size as small as 10 nm.[22–24] Using this technique, we patterned P(VDF-TrFE) copolymer films at different temperatures using molds of various patterns, with special attention paid to the effect of processing conditions on the ferroelectric properties of the imprinted films. P(VDF-TrFE) copolymers with a molar ratio of 65/35 were dissolved in dimethylformamide and spin coated onto glass substrate. Different molds were then pressed against the P(VDF-TrFE) film under an approximate pressure of 1800 psi using a Specac hydraulic press for 2 h at 130, 135, and 140 °C or 20 min at 145, 150, and 160 °C. When the imprinting temperatures are 145, 150, or 160 °C, the system is cooled to 135 °C with pressure on for 2 h. The samples were then quenched to room temperature before removing the mold. Ferroelectric hysteresis loops of imprinted P(VDF-TrFE) films were measured with radiant ferroelectric analyzer and Trek 609A high voltage amplifier. The morphology and surface potential of P(VDF-TrFE) films were measured using a Digital Instruments Dimension 3100 atomic force microscopy. The x-ray diffraction and Fourier transform infrared measurements confirmed that the spin-coated films are β phase after annealing.

Typical scanning probe microscope (SPM) image of the imprinted P(VDF-TrFE) copolymer films are shown in Figures 1(a) and 1(b) show an array of square columns (0.9 μm high and 1.5 μm wide) and gratings (0.5 μm high and 2 μm wide) in an area of 50×50 μm^2 in films around 3 μm thick, and Fig. 1(c) shows an array of 40-nm-high gratings in an area of 20×20 μm^2 in a film around 50 nm thick; the inset of Fig. 1(a) gives a closer view of the periodic array of the

a)Author to whom correspondence should be addressed; electronic mail: jjli@u.washington.edu

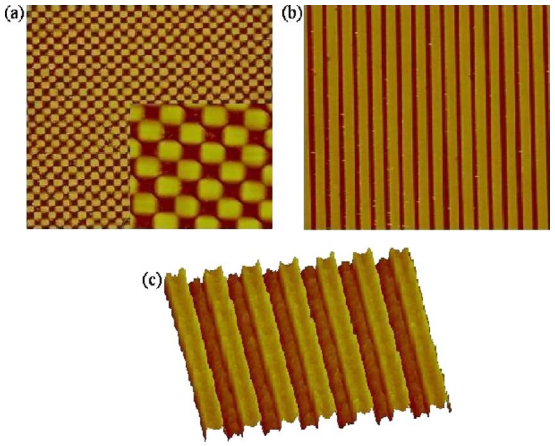

FIG. 1. (Color online) Scanning probe microscope (SPM) images of imprinted P(VDF-TrFE) films: (a) an array of square columns in 50×50 μm^2 area, the inset shows a closer view in 10×10 μm^2 area, (b) an array of gratings in 50×50 μm^2 area, and (c) an array of gratings in 20×20 μm^2.

square column in an area of 10×10 μm^2. Well-ordered arrays of micropatterns were observed in the imprinted P(VDF-TrFE) films with very few defects, even at the edges of the columns or gratings, and no variation between feature sizes in the mold and imprinted films is observed. We have not looked into the effect of pattern aspect ratio, which is limited by mechanical integrity and cannot be too high. These results demonstrate the fidelity of pattern transfer in P(VDF-TrFE) copolymer films as thin as 50 nm by microimprinting.

In microimprinting, the imprinting temperature is one of the most important processing parameters that will not only control the quality of pattern transfer but also influence the functional properties of the imprinted film. In our experiments, it is much easier to imprint the films at a temperature higher than 135 °C when a large area can be patterned with good quality. If the imprinting temperature is smaller than 130 °C, the pattern transfer into P(VDF-TrFE) films becomes very difficult due to the reduced deformability of polymers. On the other hand, the ferroelectricity of P(VDF-TrFE) is also very sensitive to the processing temperature,[25] and we have to identify an optimal processing condition for both good pattern transfer and high ferroelectricity. To this end, we spin-coated the P(VDF-TrFE) films around 3 μm thick, and an array of gratings (700 nm high and 2–5 μm wide) was then imprinted into the films at different temperatures. The ferroelectric hysteresis loops were measured on the imprinted films over a macroscopic area, which gives the averaged polarization over an area spanning both patterned and unpatterned regions. Figure 2(a) shows a characteristic hysteresis loop of P(VDF-TrFE) film imprinted at 135 °C for 2 h, and the remnant polarization is measured to be about 9.2 $\mu C/cm^2$. The variation of remnant polarization of imprinted P(VDF-TrFE) films with respect to the imprinting temperature is given in Fig. 2(b), with its inset showing a hysteresis loop of P(VDF-TrFE) film imprinted at 160 °C. It is observed that the polarization increases with imprinting temperature when it is lower than 140 °C due to the increased crystallinity of P(VDF-TrFE) films at a higher imprinting temperature. The polarization then decreases dramatically when the imprinting temperature is higher than 145 °C, since 65/35 P(VDF-TrFE) melts at about 145 °C and does not recrystallize well from the melt. As such, we

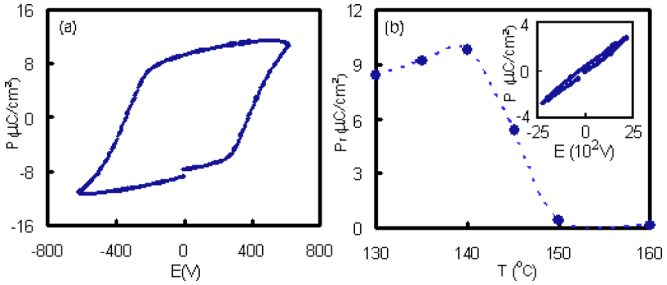

FIG. 2. (Color online) Ferroelectric properties of imprinted P(VDF-TrFE) films. (a) Hysteresis loop of P(VDF-TrFE) film imprinted at 135 °C for 2 h. (b) The variation of remnant polarization of P(VDF-TrFE) films (measured at room temperature) with respect to the imprinting temperature; the inset shows a hysteresis loop of P(VDF-TrFE) film imprinted at 160 °C.

conclude that 140 °C is the optimal imprinting temperature for β-phase ferroelectric P(VDF-TrFE) films.

The hysteresis measurement only gives us averaged polarization over macroscale area, and we resolve the surface potential measurement by SPM to investigate the local ferroelectric properties of the imprinted structure at microscale. According to Kajiyama *et al.*[26] and Chen *et al.*,[27] there is an intimate correlation between the field-induced polarization and the surface potential in the poled area of ferroelectric thin films, and the surface charge could be stabilized by spontaneous polarization, leading to higher surface potential for higher polarization. As such, we imprinted an array of 40-nm-high grating in P(VDF-TrFE) films around 50 nm thick at different temperatures. A conductive tip of SPM is then used to apply a dc voltage of 10 V to a 1×1 μm^2 area in a particular grating, and a locally poled area is formed. The surface potential is then measured in the subsequent scan. Before poling the local area, it has been verified that the surface potential is uniform. Figure 3 shows a simultaneously obtained topographical image and surface potential mapping of the P(VDF-TrFE) film imprinted at 140 °C. The height and width of the grating are observed to be about 40 nm and 1.5 μm, respectively, and the center of the image showing an area of 1×1 μm^2 with four blur edges is the poled area. The surface potential distribution around the poled area 27 min after poling is shown in Fig. 3(b), and higher surface potential is observed in the poled area shown in the bright region, with the potential difference approxi-

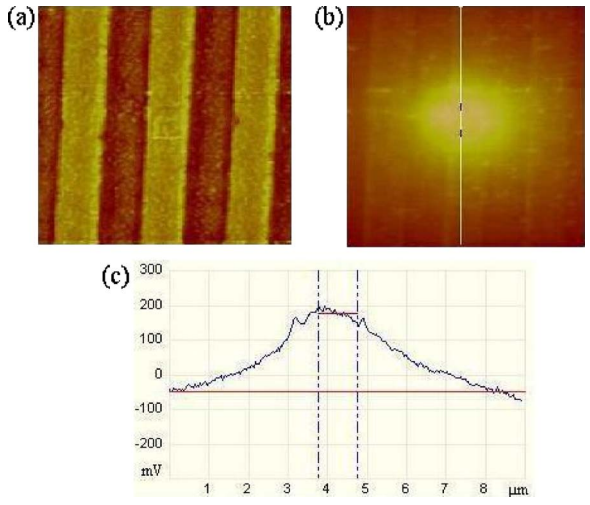

FIG. 3. (Color online) Surface potential distribution of imprinted P(VDF-TrFE) films, (a) surface morphology, (b) surface potential distribution, and (c) position dependence of the surface potential along the solid line in (b).

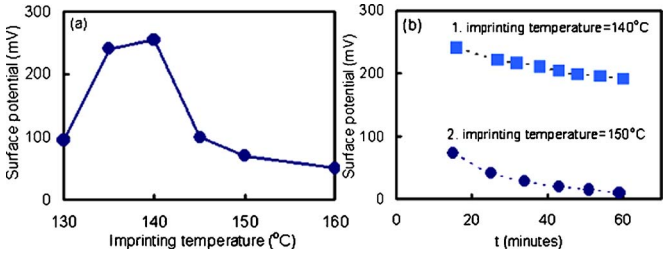

FIG. 4. (Color online) The variation of surface potential (a) with respect to imprinting temperature and (b) with respect to the time after poling; their imprinting temperatures are 140 and 150 °C, respectively.

mately 220 mV. The area is positively poled such that the dipoles are oriented downward. The position dependence of the surface potential along the solid vertical line of Fig. 3(b) is shown in Fig. 3(c), in which the poled area is between the two dashed lines. As observed in Figs. 3(b) and 3(c), the boundary between poled and unpoled areas in the image is not so clear.

In order to understand the correlation between the surface potential and polarization, we have to consider the distribution of electric charges in a poled film.[28,29] When a positive voltage was applied to the film from the tip, holes emitted from the cantilever can be trapped on the surface of the P(VDF/TrFE) film while the polarization points toward the bottom electrode. The polarization induces polarization charges on the top surface of the film that is negative, which stabilizes the positively charged holes,[28,29] resulting in positive surface potential measured from the poled area, as we observed in Figs. 3(b) and 3(c). To further verify the correlation between spontaneous polarization and surface potential, we measured the surface potential in patterned P(VDF-TrFE) films imprinted at different temperatures, as shown in Fig. 4(a), 15 min after poling. All the data are averaged from the poled area of P(VDF-TrFE) grating, and it is observed that the surface potential increases with the imprinting temperature when it is lower than 140 °C and decreases dramatically above 145 °C. This correlates with polarization-temperature curve in Fig. 2(b) very well, where higher polarization generally corresponds to higher surface potential, suggesting that the imprinted P(VDF-TrFE) films as thin as 50 nm maintain good ferroelectricity and show similar temperature characteristics as the bulk films. This is further confirmed by the time dependence of the surface potential after poling in two patterned P(VDF/TrFE) films imprinted at 140 °C (film 1) and 150 °C (film 2), respectively. The surface potential of film 1 is about 240 mV 15 min after poling and 191 mV 60 min after poling, about 20% reduction, suggesting that the trapped surface charges are stable, thanks to the large polarization in the film imprinted at 140 °C. On the other hand, the surface potential of film 2 is about 70 mV 15 min after poling and 9 mV 60 min after poling, about 87% reduction, suggesting that the trapped surface changes are rather unstable due to much smaller polarization in the film imprinted at 150 °C. These results are consistent with surface potential measurement in ferroelectric lead zirconic titanate and paraelectric polyethylene.[27]

In conclusion, β-phase ferroelectric P(VDF-TrFE) copolymer films have been patterned by microimprinting. Various patterns have been created with good pattern transfer between the molds and films. Ferroelectricity of the imprinted films has been confirmed by ferroelectric hysteresis and surface potential measurement, and very good correlation was observed between remnant polarization and surface potential of the imprinted films. Imprinted P(VDF-TrFE) films show high remnant polarization and high poling-induced surface potential when the imprinting temperature is around 140 °C, suggesting that 140 °C is the optimal imprinting temperature for P(VDF-TrFE) films. The patterned ferroelectric P(VDF-TrFE) films can be used in a wide range of applications.

The work is supported by National Science Foundation (DMR-0706100 and CMMI-0727922), Bryan T. McMinn Endowed Professorship in Mechanical Engineering, and by the Nebraska Research Initiative. The SPM characterizations were carried out at University of Washington NanoTech User Facility, a member of the National Nanotechnology Infrastructure Network supported by National Science Foundation.

[1] A. V. Bune, V. M. Fridkin, S. Ducharme, L. M. Blinov, S. P. Palto, A. V. Sorokin, S. G. Yudin, and A. Zlatkin, Nature (London) **391**, 874 (1998).
[2] S. Ducharme, V. M. Fridkin, A. V. Bune, S. P. Palto, L. M. Blinov, N. N. Petukhova, and S. G. Yudin, Phys. Rev. Lett. **84**, 175 (2000).
[3] Q. M. Zhang, V. Bharti, and X. Zhao, Science **280**, 2101 (1998).
[4] X. Z. Zhao, V. Bharti, Q. M. Zhang, T. Romotowski, F. Tito, and R. Ting, Appl. Phys. Lett. **73**, 2054 (1998).
[5] B. J. Chu, X. Zhou, K. L. Ren, B. Neese, M. R. Lin, Q. Wang, F. Bauer, and Q. M. Zhang, Science **313**, 334 (2006).
[6] B. D. Gates, Q. B. Xu, M. Stewart, D. Ryan, C. G. Willson, and G. M. Whitesides, Chem. Rev. (Washington, D.C.) **105**, 1171 (2005).
[7] Y. Chen and A. Pépin, Electrophoresis **22**, 187 (2001).
[8] C. R. K. Marrian and D. M. Tennant, J. Vac. Sci. Technol. A **21**, 207 (2003).
[9] S. Clemens, T. Schneller, A. V. D. Hart, F. Peter, and R. Waser, Adv. Mater. (Weinheim, Ger.) **17**, 1357 (2005).
[10] U. P. Schönholzer, R. Hummel, and L. J. Gauckler, Adv. Mater. (Weinheim, Ger.) **12**, 1261 (2000).
[11] S. Seraji, Y. Wu, N. E. Jewell-Larson, M. J. Forbess, S. J. Limmer, T. P. Chou, and G. Z. Cao, Adv. Mater. (Weinheim, Ger.) **12**, 1421 (2000).
[12] C. Canalias, V. Pasiskevicius, R. Clemens, and F. Laurell, Appl. Phys. Lett. **82**, 4233 (2003).
[13] Y. J. Park, Y. S. Kang, and C. Park, Eur. Polym. J. **41**, 1002 (2005).
[14] Z. J. Hu, G. Baralia, V. Bayot, J. F. Gohy, and A. M. Jonas, Nano Lett. **5**, 1738 (2005).
[15] S. J. Kang, Y. J. Park, J. Hwang, H. J. Jeong, J. S. Lee, K. J. Kim, H. C. Kim, J. Huh, and C. Park, Adv. Mater. (Weinheim, Ger.) **19**, 581 (2007).
[16] R. G. Kepler and R. A. Anderson, Adv. Phys. **41**, 1 (1992).
[17] M. J. Bai and S. Ducharme, Appl. Phys. Lett. **85**, 3528 (2004).
[18] M. J. Bai, M. Poulsen, and S. Ducharme, J. Phys.: Condens. Matter **18**, 7383 (2006).
[19] J. Y. Li, Y. Luo, M. J. Bai, and S. Ducharme, Appl. Phys. Lett. **87**, 213116 (2005).
[20] J. Y. Li, Y. Luo, M. J. Bai, and S. Ducharme, J. Mech. Phys. Solids **54**, 2162 (2006).
[21] J. Choi, H. M. Manohara, E. Morikawa, P. T. Sprunger, P. A. Dowben, and S. P. Palto, Appl. Phys. Lett. **76**, 381 (2000).
[22] S. Y. Chou, P. R. Krauss, and P. J. Renstrom, Appl. Phys. Lett. **67**, 3114 (1995).
[23] S. Y. Chou, P. R. Krauss, and P. J. Renstrom, J. Vac. Sci. Technol. B **14**, 4129 (1996).
[24] S. Zankovych1, T. Hoffmann, J. Seekamp, J.-U. Bruch, and C. M. Sotomayor Torres, Nanotechnology **12**, 91 (2001).
[25] Y. J. Park, S. J. Kang, C. Park, K. J. Kim, H. S. Lee, M. S. Lee, U.-I. Chung, and I. J. Park, Appl. Phys. Lett. **88**, 242908 (2006).
[26] T. Kajiyama, N. Khuwattanasil, and A. Takahara, J. Vac. Sci. Technol. B **16**, 121 (1998).
[27] X. Q. Chen, H. Yamada, T. Horiuchi, K. Matsushige, S. Watanabe, M. Kawai, and P. S. Weiss, J. Vac. Sci. Technol. B **17**, 1930 (1999).
[28] L. M. Blinov, R. Barberi, S. P. Palto, M. P. De Santo, and S. G. Yudin, J. Appl. Phys. **89**, 3960 (2001).
[29] M. P. De Santo, R. Barberi, L. M. Blinov, S. P. Palto, and S. G. Yudin, Mol. Mater. **12**, 329 (2000).